J Incl Phenom Macrocycl Chem (2007) 58:295–305
DOI 10.1007/s10847-006-9157-3

ORIGINAL PAPER

Rationalizing some experimental facts on the complexation of 2-methyl naphthalenecarboxylate and hydroxypropyled cyclodextrins by molecular mechanics and molecular dynamics

Antonio Di Marino · Francisco Mendicuti

Received: 3 October 2006 / Accepted: 30 October 2006 / Published online: 6 December 2006

Abstract Molecular mechanics (MM) and Molecular dynamics (MD) calculations were applied to study the complexation of 2-Methyl naphthalenecarboxylate (2MN) and 2-hydroxypropyl -α-, -β-, and γ-cyclodextrins (HPCDs) in the presence of water. Results showed that 1:1 complexes of 2MN with modified cyclodextrins are stable and that the non-bonded van der Waals interactions are mainly responsible for the complexation. Theoretical results are in good agreement with fluoresence results and they permit us to explain the signs and quantitative differences of ΔH^0 and ΔS^0 on the basis of the different cavity sizes and the movement of the guest inside the HPCD cavity. Results also reveal a more favorable complexation when 2MN approaches on its polar side.

Keywords Cyclodextrins · 2-methyl naphthalenecarboxylate · Molecular mechanics · Molecular dynamics

Introduction

Cyclodextrins (CDs) are cyclic oligosaccharides composed of a few D-(+)-glucopyranose units joined by α-(1,4)-linkages. CDs have the ability to form inclusion complexes by non-covalent binding with a variety of guest molecules in their internal cavities, which apparently exhibit more hydrophobic character than the surrounding aqueous environment. The complexation process in solution seems to depend mainly on the size, shape and hydrophobicity of the guest molecule relative to the host cavity. Several types of interactions are proposed as driving forces for the inclusion process, such as van der Waals between guest and host, hydrogen bonding between the guest and the hydroxyl groups of CDs, the release of strain energy in the macromolecular ring of the CD, dipole–dipole and/or electric charge interaction, the release of enthalpy-rich water inside the cavity, etc. [1–5]. Chemical modification of a natural unsubstituted CD alters its properties and subsequently the thermodynamics of the association with a specific guest.

The application of Molecular Mechanics (MM) and Molecular Dynamics (MD) techniques to CD complexation with small and large molecules can provide valuable information about the stoichiometry, complex geometry and the driving forces responsible for such processes, thus strengthening the thermodynamics accompanying such processes [6–39]. Our group has also contributed to this kind of studies [40–48].

In a previous experimental work [49], different fluorescence techniques were used to study inclusion complexes of 2-methyl naphthalenecarboxylate (2MN) with 2-hydroxypropyl-α-, -β-, and γ-cyclodextrins (HPCDs) (molar substitution, MS = 0.6 and mostly substituted at position 2 of the glucopyranose unit according to Aldrich specifications). The formation constant, the stoichiometry and the thermodynamic parameters ΔH^0 and ΔS^0 accompanying the complexation processes were investigated by obtaining the variation of the intensity ratios of two fluorescence emission bands (R), which were very sensitive to the medium polarity, with [HPCD] and temperature. Experiments showed that 2MN formed

A. D. Marino · F. Mendicuti (✉)
Departamento de Química Física, Universidad de Alcalá, 28871 Alcalá de Henares, Madrid, Spain
e-mail: francisco.mendicuti@uah.es

thermodynamically stable complexes of 1/1 stoichiometry with α-, β-, and γ-HPCDs. Formation constants at 25°C were 780, 2,700, and 165 (M), respectively [49]. Constants for the complexes with α- and β-HPCDs were larger than those ones for complexes formed with their unsubstituted naturally occurring counterparts α- and β-CDs [50]. However, similar values were obtained for both complexes of 2MN with γ-HPCD and γ-CD [42, 49]. As with the unsubstituted CDs, enthalpy variation upon complexation was more favorable as the HPCD size decreased. They were -24.7, -7.6, and +6.3 kJ/mol for 2MN complexation with α-, β-, and γ-HPCD, respectively. These values were also less favorable than the ones obtained for 2MN complexation with their unsubstituted CDs counterparts [42, 50]. Entropy changes reported for 2MN complexation with α-, β-, and γ-HPCDs were -28.3, +39.8, and +63.3 J k/mol, respectively. With the same signs, however, entropy variations were more favorable or less unfavorable to complexation than with unmodified α-, β-, and γ-CDs [42, 50]. These quantitative differences in thermodynamics parameters of α-, β-, and γ-HPCD and with respect to the natural CDs seem to be due to the different cavity sizes [49].

The analysis of fluorescence quenching measurements suggested a similar location the 2MN guest when complexed with any of the HPCDs. The 2MN seems to penetrate inside any of the three HPCD cavities [49]. These cavities, in contrast to the unsubstituted CDs [42, 50], have similar polarities ($\varepsilon \approx 50$) [49]. The fluorescence anisotropy values when 2MN was complexed were also considerably larger for the 2MN/α-HPCD than for the complexes of 2MN with the other two HPCDs. This, in agreement with the sign of entropy changes, suggested that the movement of the 2MN guest when it was included in β- and γ-HPCD cavities should only be moderately hindered, whereas as 2MN should fit more tightly inside the α-HPCD, such movements should be hindered. The possibility of some kind of 2MN and α-HPCD interactions (hydrogen bond type), which should contribute in the same way, was also proposed from these results and from the analysis of fluorescence lifetimes. The 2MN when complexed with α-HPCD, contrary to other complexes, shows a shorter fluorescence lifetime than when it is free [49]. Results also suggested that van der Waals attractive interactions could be mainly responsible for 2MN complexation with any of the CDs studied, with the the hydrophobic forces playing a minor role.

In the present work MM and MD studies on 2MN and HPCDs inclusion complexes, mainly in the presence of water molecules were performed by using the Tripos Force Field [51]. With this work we aim to give an explanation of the formation constants, the differences in thermodynamics parameters associated to the complexations and their relationship with the geometry of complexes formed, as well as to obtain more information on the possible driving forces behind such inclusion processes.

Theoretical details

The 1/1 stoichiometry complexes studied were between the HPCDs fully substituted at C2 of the glucopyranose unit (MS = 1.0) and the 2MN guest. MM and MD calculations were mainly performed in the presence of water molecules to simulate aqueous medium. The conformations generated by MM and the MD trajectories were obtained by using Sybyl 6.9 from Tripos Associates (St. Louis, MO, USA) [52]. The potential energy of each system was evaluated as the sum of five contributions: bond stretching, bond angle bending, torsion potentials, van der Waals, and electrostatic interactions and out of plane. Calculations were performed at $\varepsilon = 1$ (relative permittivity) for the electrostatic interactions. Charges for the guests and water used previously [40, 42] were obtained by MOPAC (AM1) [53]. Charges for HPCD were also obtained by same method, by separately obtaining charges for the CD core [40–48] and for the 2-hydroxypropyl (HP) substituent (in the all-trans conformation). HP substituent charges were rescaled before attaching them to the CD to give HPCDs with zero net charge. Extended non-bonded cut-off distances were set at 8 Å for van der Waals and electrostatic interactions. Minimization of the potential energy of the system was performed by the simplex algorithm and the conjugate gradient was used as termination method [54, 55]. In the presence of water (in the vacuum) the termination gradients were 1 kcal/molÅ (0.2 kcal/molÅ) for MM calculations and 0.5 kcal/molÅ for the starting conformation used for MD. Water molecules were added to the host-guest systems with the Molecular Silverware algorithm (MS) [56]. Periodic boundary conditions (PBC) were also employed.

Binding guest–host energy ($E_{binding}$) for a particular system was obtained by subtracting the sum of the potential energies of isolated guests and CD from the potential energy of the guest/CD system. The water solvent molecules were previously removed from the box. Any host–guest interaction was obtained in a similar manner. A measure of the loss or gain of the HPCD ring strain energy upon complexation was evaluated by taking into account bond stretching, bond angle bending, and torsion energy terms. A hydrogen

bond is assumed when the O···H-O angle is in the range 120–180° and the O···H distance is between 0.8 and 2.8 Å.

As previously, the initial structure of the 2MN guest was built so that the ester and aromatic ring groups were coplanar [40, 42]. The modified HPCD was initially built in the undistorted form [40–48] where the glycosidic oxygen atoms were in the same plane, the torsion angles ϕ and ψ were 0° and –3°, respectively, the bond angles τ for the 1,4 linkages were fixed at 130.3, 121.7, and 115.3° for α-, β-, and γ-HPCDs, respectively, and χ-side chain torsional angles were in trans. HP substituents at glucopyranose C2 were also placed in the most extended conformation.

Molecular mechanics

For 1/1guest inclusion processes, each HPCD was initially placed so that the center of mass of the glycosidic oxygen atoms (denoted by o in Fig. 1) was located at the origin of a coordinate system with its axis oriented as depicted in Fig. 1. The host–guest distance was measured as the oo' projection on the y coordinate. The inclusion torsion angle θ was measured between the yz and oo'C9 (C9 from naphthalene group) planes. The oo'C9 angle, ε, also defines the orientation of 2MN relative to the y-axis.

All the MM calculations reported below were performed where 2MN approached the HPCD by the polar (P) (as depicted in Fig. 1) and non-polar (NP) sides. In order to obtain the most favorable approach of the guest, binding energies of all the optimized structures in the vacuum obtained by scanning ε and θ angles, in the 10–100° and 0–55° ranges, respectively, both at 10° intervals and the coordinate y (oo' distance) from +10 to –6 Å at 2 Å intervals were achieved. Critical analysis revealed optima ε and θ pairs of angles of approximately: 70°; 5° (90°; 55°), 60°; 5° (90°; 46°), and 50°; 0° (90°; 40°) for P (NP) 2MN approaching to α-, β-, and γ-HPCDs, respectively.

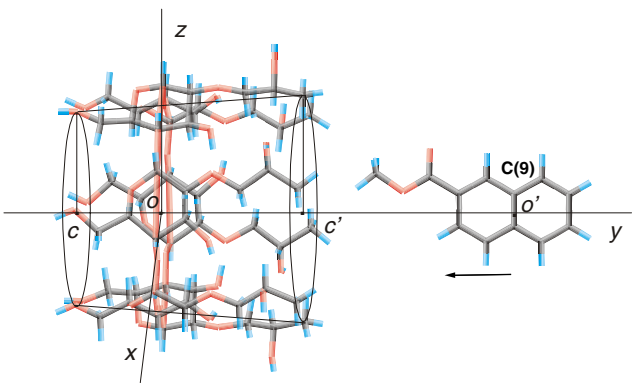

Fig. 1 Coordinate system used to simulate the complexation process of the host (HPCD) and the guest (2MN) molecules

With fixed ε and θ angles, the 1:1 complexation was emulated by approaching the guest to the HPCD by the wider HP group side in small steps of 1 Å along the y coordinate from 20 up to –20 Å. Water molecules were added to each of the structures generated. These were optimized (PBC, gradient 1 kcal/molÅ) and saved for further analysis. Henceforth, we will refer to the guest with α-, β-, and γ-HPCD complexation by the 2MN polar (non-polar) side as AP (ANP), BP (BNP), and GP (GNP), respectively.

Molecular dynamics

Molecular dynamics trajectories in the presence of water were performed starting from the structures of minimal binding energy (MBE) obtained in the previous MM calculations, which were minimized once again before starting MD (gradient of 0.5 kcal/molÅ). PBC conditions were also used. Bonds where H atoms were involved were constrained from vibrating; other conformational parameters were variable. MD trajectories of the systems were performed at 300 K. Starting from 1 K, the temperature was increased by 20° intervals and the whole system equilibrated at each temperature for 500 fs up to reaching 300 K. This heating/equilibration period was discharged from the analysis. From this point, a short trajectory of 250 ps (integration time step 2 fs) was simulated. The velocities were rescaled at 10 fs intervals. Conformations were saved every 250 fs, yielding 1,000 images per trajectory for subsequent analysis. The average of any property obtained from the analysis of MD, was calculated by equally weighing each image.

Results and discussion

Molecular mechanics

Figure 2 shows the variation of $E_{binding}$, van der Waals and electrostatic contributions obtained by scanning y from 20 to –10 Å at 1 Å intervals when 2MN approaches HPCDs by the polar and non-polar sides, respectively. Calculations suggest that the complexation processes are favorable. Structures of MBE were reached at approximately y (in Å) = +3.0 (+4.1), +2.5 (–1.0), and + 1.8 (0.3) for AP (ANP), BP (BNP), and GP (GNP) systems, respectively. $E_{binding}$ values at the coordinate of MBE, which were also collected in Tables 1 and 2, were –94.0 (–63.5), –65.2 (–67.2), and

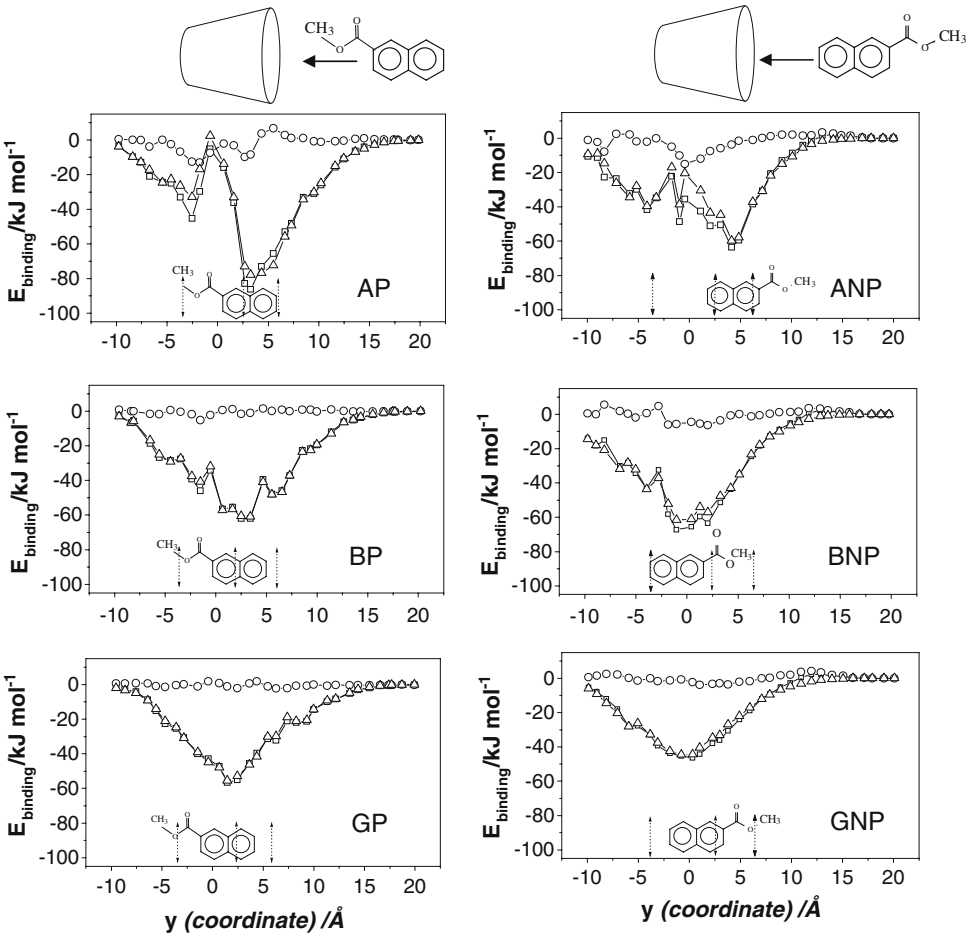

Fig. 2 Variation of $E_{binding}$ (squares), van der Waals (triangles), and electrostatic (circles) contributions obtained by scanning *y* from 20 to –10 Å at 1 Å intervals when 2MN approaches HPCDs on the polar (AP, BP, GP) (left pannels) and non-polar (ANP, BNP, GNP) (right pannels) sides, respectively. Scheme of the placement of 2MN at the MBE. Dashed lines correspond to the y coordinates of the center of mass of primary oxygens (–3.6 Å), secondary ones at C3 (+2.5 Å), and methyl carbons of HP groups (+6.3 Å) of undistorted HPCDs

–57.2 (46.5) kJ/mol, respectively. When 2MN approaches on the polar side, $E_{binding}$ values at the MBE become more negative as the HPCD macroring size decreases, following the same trend as the experimental ΔH^0, which becomes more negative when going from γ- to β- and α-HPCDs. This behavior, due to the fact that a good portion of 2MN is outside the α-HPCD cavity at the MBE, is not observed for the NP guest approach. Generally, the results are more favorable for the formation of the complex upon approaching on the polar side. Exceptions are BP and BNP systems, whose MBE are very similar. Most of the $E_{binding}$ is due to van der Waals host–guest interactions at any y coordinate for any guest–host complexation processes. The electrostatic interactions hardly change upon complexation and they are only slightly significant at the MBE for AP (13% of MBE), ANP (6%), and BNP (8%).

As shown in a schematic way in Fig. 2, the 2MN guest penetrates inside most of the HPCD cavities. The exception is ANP where the 2MN naphthalene is close to the rim of C atoms from the terminal methyl of HP group and the ester group mostly outside the cavity. It is, however, relevant that when the guest approaches on the polar side, the naphthalene ring and ester group of 2MN are placed at similar y coordinate. Both are close to the y coordinate of the glucopyranose secondary OH(3) and to the primary OH groups (at C6) rims, respectively. This fact should agree with the experimental quenching [49] measurements that pointed out similar media surrounding the 2MN guests, with comparable polarities ($\varepsilon \approx 50$), when they complex with any of the HPCDs.

ε_{min}, θ_{min} angle pairs at the MBE were 71.6°,1° (90.0°,55.8°); 57.9°,8.9° (77.5°,55.1°), and 43.2°,11.0° (119.8°, 32.3°) for AP (ANP), BP (BNP), and GP (GNP) systems, respectively. They did not vary much from the initial values. The total potential energy E_{tot} of the complexes as a function of the y coordinate, as well as several contributions, electrostatics, van der Waals, and strain energy are depicted in Fig. 3 for P systems. Similar plots, not shown here, were obtained for NP ones.

Complexation causes a slight decrease in the total potential energy for the systems studied. Mainly responsible for such decreases are the non-bonded van der Waals interactions, although they are not the

Table 1 Binding energy and selected components (kJ/mol) at the minimum energy (MBE), subscript 0, and at the largest separation (y = +20) of guest and host, subscript ∞, for AP, BP, and GP systems

Energy (kJ/mol)	AP_0	AP_∞	BP_0	BP_∞	GP_0	GP_∞
$E_{binding}$	–94.1	–0.2	–65.2	–0.1	–57.2	–0.1
Electrostatic part	–12.2	–0.0	–3.3	–0.1	–1.9	–0.1
van der Waals part	–81.8	–0.2	–62.0	–0.0	–55.3	–0.0
$E_{int\ HPCD–2MN\ naphthalene}$	–60.1	0	–49.0	0	–39.4	0
Electrostatic part	–5.8	0	–1.4	–0.0	0.6	0.0
van der Waals part	–54.3	0	–47.6	0	–40.0	–0.0
$E_{int\ HPCD–2MN\ ester\ group}$	–33.9	–0.0	–16.2	–0.1	–17.8	–0.1
Electrostatic part	–6.4	0.1	–1.9	–0.1	–2.5	–0.1
van der Waals part	–27.4	–0.1	–14.3	–0.0	–15.4	–0.0
E_{tot} guest : host	442.5	523.4	584.9	625.9	673.0	717.5
Electrostatic part	92.2	102.8	117.0	126.2	148.2	134.6
van der Waals part	–76.9	4.0	–17.3	42.3	–3.9	56.7
Strain energy	427.6	416.1	482.3	455.9	526.1	522.6
E_{tot} host	462.2	456.6	570.6	554.3	654.6	643.9
Electrostatic part	67.4	66.1	82.3	88.1	113.2	97.3
van der Waals part	–9.7	–8.6	30.0	29.5	35.1	43.0
Strain energy	404.5	399.0	458.2	436.7	506.3	503.6
E_{tot} guest	74.4	66.9	79.6	71.7	75.6	73.7
Electrostatic part	37.1	36.7	38.0	38.1	36.9	37.4
van der Waals part	14.6	12.8	14.5	12.8	16.3	13.8
Strain energy	21.2	17.1	24.1	19.2	19.8	19.0

largest contributions to E_{tot}. The electrostatics interactions hardly change upon complexation. The strain energy is the main contribution to E_{tot} and it slightly increases (decreases) upon the P (NP) approaching of the guest. These results contrast with the ones previously obtained for complexation of 2MN with the unsubstituted natural occurring α- and β-CDs. Nevertheless, these results were only performed on the basis of the NP guest to host approaching [40, 42]. The 2MN complexation with natural non-substituted α- and β-CDs makes E_{tot} increase, becoming larger as the CD macroring size decreases. Strain term contributes most to this increase and there is only a little contribution to it from van der Waals and electrostatics [40]. Complexation of 2MN with unsubstituted γ-CD, however, behaved like 2MN with HPCDs, whose results

Table 2 Binding energy, and selected components (kJ/mol) at the minimum energy (MBE), subscript 0, and at the largest separation (y = +20) of guest and host, subscript ∞, for ANP, BNP, and GNP systems

Energy (kJ/mol)	ANP_0	ANP_∞	BNP_0	BNP_∞	GNP_0	GNP_∞
$E_{binding}$	–63.5	0.0	–67.2	0	–46.5	0
Electrostatic part	–3.8	0	–5.6	0	–2.2	0
van der Waals part	–59.7	0.0	–61.7	–0.0	–44.3	0
$E_{int\ HPCD–2MN\ naphthalene}$	–52.8	0	–49.4	0	–34.5	0
Electrostatic part	1.5	0.0	–3.9	0	1.2	0
van der Waals part	–54.3	0	–45.6	–0.0	–35.7	0
$E_{int\ HPCD–2MN\ ester\ group}$	–10.7	0	–17.8	0	–12.0	0
Electrostatic part	–5.3	0.0	–1.7	0	–3.4	0
van der Waals part	–5.4	0	–16.1	0	–8.6	0
E_{tot} guest : host	507.6	560.1	577.8	627.4	672.1	745.0
Electrostatic part	102.3	112.9	126.5	130.7	158.4	149.3
van der Waals part	–19.6	18.3	–17.4	20.1	1.6	52.2
Strain energy	424.0	427.5	467.7	475.0	510.7	542.5
E_{tot} host	492.1	477.9	570.0	543.9	649.1	659.9
Electrostatic part	68.3	76.1	95.1	94.4	122.7	111.8
van der Waals part	25.1	4.1	30.9	7.9	35.3	40.7
Strain energy	398.7	397.8	444.0	441.6	491.1	507.4
E_{tot} guest	79.0	82.2	75.0	83.5	69.6	87.1
Electrostatic part	37.8	36.8	36.9	36.3	37.9	37.5
van der Waals part	15.0	14.2	13.3	12.6	10.7	11.5
Strain energy	25.3	29.7	23.7	33.4	19.6	35.1

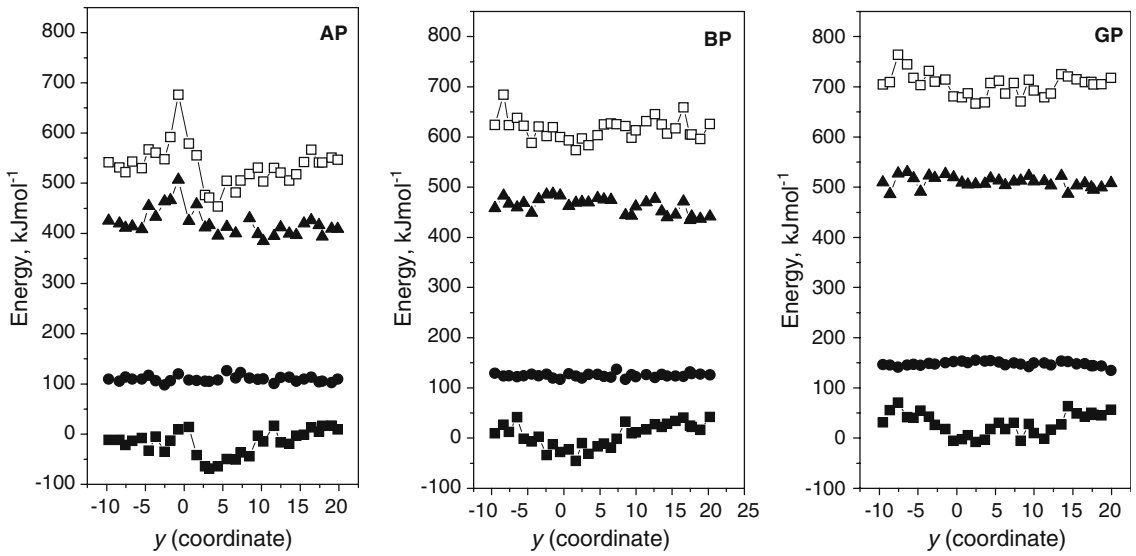

Fig. 3 Total potential energy (open squares), van der Waals (filled circles) and electrostatics (filled squares), and strain energy (filled triangles) contributions versus the *y* coordinate for AP, BP, and GP systems

are probably derived from the flexibility and the repulsion of HP groups. This makes the entrance into the cavity a little wider on this side and slightly narrower on the opposite one when compared to their natural counterparts. The analysis of MD calculations on α-, β-, γ-HPCDs in the vacuo with different molar substitutions reaches similar conclusions (F. Mendicuti, unpublished data).

Figure 4 shows the interactions between the naphthalene (N) and ester (E) groups of the guest and HPCDs as a function of the host/guest distance along the y coordinate for polar approaching systems. Both interactions were found to be negative and they contributed to the stabilization of the systems, the N/host always being the stronger one. The same observations can be extended to NP systems. The exception is AP where the N/α-HPCD interactions have a relatively wide unfavorable gap around $y = 0$, which is also observed to a smaller extent for ANP. The AP system also presents some additional characteristics that do not appear in the other P and NP systems: (1) both E/α-HPCD and N/α-HPCD interactions simultaneously show the minimum values at the y coordinates of the MBE and (2) the contribution due to E/host interaction, although smaller than the N/host one, represents more than one-third of the total binding energy.

Tables 1 and 2 also collect data on interaction energies between relevant groups of 2MN (N and E) and HPCD hosts for the conformations of MBE and at infinite host-guest distance. Results corroborate that the largest contribution to MBE comes from the interaction of the host with the N groups. However, it is significant that for the AP system almost 36% of MBE is due to the E/α-HPCD interaction (44% of it is due to the interaction with the tails substituted at C5). This interaction involving the ester group, which is relatively smaller for B and C (P as well as NP) systems, is generally larger for P approaching complexes. The exception is for 2MN : β-HPCD whose results for BP and BNP are very similar.

Figure 5 shows the structures for the MBE for AP, BP, and GP complexes.

Molecular dynamics

Figure 6 depicts the y coordinate of the center of mass of the naphthalene ring during the 250 ps MD trajectories for P and NP systems, which were initially placed at the conformations of MBE obtained by MM, with the hosts centered at $y = 0$. Dotted lines in Fig. 6 show the y coordinate of the planes that contain: (a) the C atoms of methyl end groups of hydroxypropyl chains ($y = +6.3$ Å); (b) the bridging O atoms ($y = 0$); and (c) the oxygens of primary OH at the opposite side ($y = -3.6$ Å) for the undistorted hosts.

With the exception of a few conformations of BP and GP, and some more for GNP, the center of mass of the naphthalene ring for the 2MN guests stay inside the cavity throughout the whole MD trajectory. Results, which are related to the differences of binding energies upon complexation, show that the center of mass of the 2MN naphthalene ring prefers to locate very close to the y coordinate of the initial conformation for AP and ANP systems. However, with other systems, for which the HPCD cavities are larger, the 2MN guest can move a little more freely along this coordinate from the

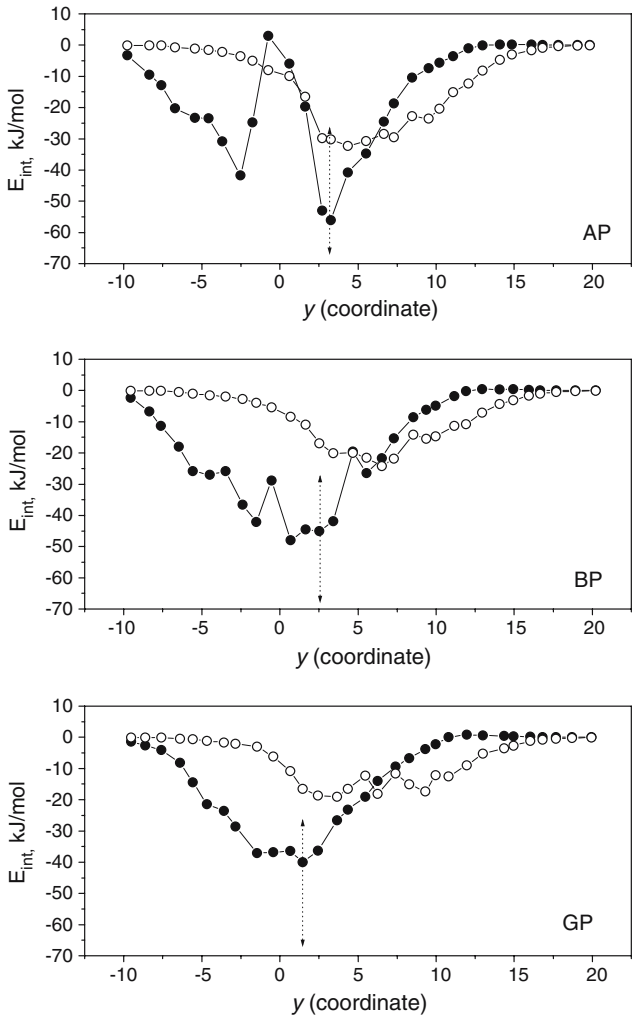

Fig. 4 Interaction energy between naphthalene (filled circles) and ester (open circles) groups of 2MN and HPCDs versus *y* coordinate for AP, BP, and GP systems

initial MBE structures. The 2MN almost leaves the cavity during the last portion of the MD trajectories for GNP and GP systems from opposite sides. When 2MN approaches HPCD on the non-polar side, the ester group is either placed near the entrance of the cavity (BNP) or totally outside it (ANP and GNP) during most of the MD trajectory.

Figure 7 shows the instantaneous xz plane projections, seen from the positive y coordinate side, of the placement of carboxylic oxygen and H5 (bonded to C5 of naphthalene) atoms of the 2MN guest for all the systems studied during MD. Dotted lines in Fig. 7 correspond to the location of the bridging oxygen atoms rim for the non-distorted α-, β-, and γ-HPCDs with radii of ~4.4, 5.2, and 5.9 Å, respectively. These projections are mainly affected by rotation of the 2MN guest inside the HPCD cavity, but they also change by the fluctuation of the bonds. The results apparently indicate that the mobility of 2MN inside the cavity becomes smaller as the cavity size decreases. Exceptions to such observed behavior are the increase in mobility of H5 for BP, and carboxylic oxygen for ANP, BNP, and GNP. These exceptions are derived from the placement of those atoms that are located outside the CD during most of the trajectory. When such atoms are placed outside the cavity the mobility, as expected, noticeably increases. What is significant is the low mobility for AP, where the ester group seems to be located quite close to the primary hydroxyl groups rim of α-HPCD during the whole MD trajectory. The interaction involving the ester group pointed out in the previous section contributes to this special characteristic.

The movement of the guest inside the cavity was also studied by analyzing the time evolution of *x, y*, and *z* coordinates of heavy atoms of 2MN guest (excluding hydrogen atoms) relative to the HPCD. $y(t,j)$ denote the instantaneous value at time t of the y coordinate on atom j. The instantaneous rate of change in the y coordinate of each atom j was defined as the simple average obtained from 1,000 MD structures separated in time by $\Delta t = 0.25$ ps according to:

$$\frac{\Delta y_j}{\Delta t} = \frac{\left\langle \left| y_{t,j} - y_{(t-\Delta t),j} \right| \right\rangle}{\Delta t} \quad (1)$$

A new average over all carbon and oxygen atoms of 2MN guest, $\left(\left\langle \Delta y_j \right\rangle / \Delta t\right)$, gives the average of the instantaneous rate of change of the y coordinate for such atoms relative to the HPCD during the MD trajectory. This rate is related to the translational motion of the guest along the y coordinate. The average of the instantaneous rates of variation of x and z coordinates, which are associated to the 2MN rotation motion inside the cavity, were obtained in a similar way. Results are collected in Table 3 for all systems studied. Values obtained for AP, BP, and GP systems indicate, as expected, that the mobility, translation along the y-axis or rotation inside the cavity, of 2MN is smaller when it is confined within the narrow α-HPCD cavity than when it is inside the β- or γ-HPCDs. Results obtained for NP approaching guests to HPCDs are, however, a little different. They are more conditioned to the location of the ester groups that are close to the cavity entrance of the HP groups side or outside it. In this case, the largest motion of the guest is for ANP and GNP systems where ester groups are totally outside the cavity.

Table 4 (rows 2–4) lists the average coordinate y of the center of mass of the naphthalene ring, as well as the θ and ε angles that define the relative orientation of

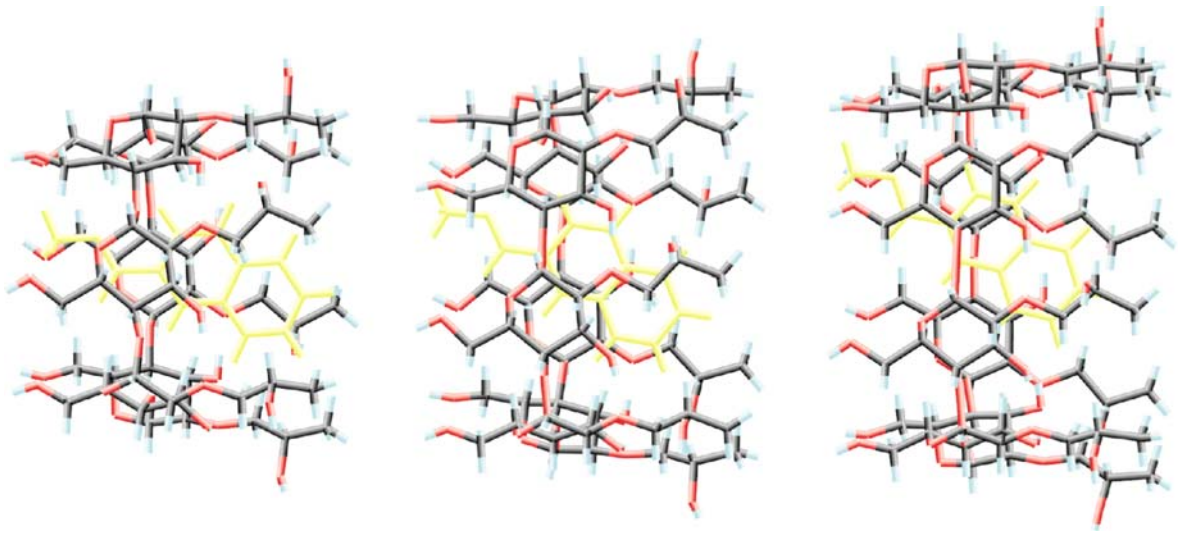

Fig. 5 Side views of the structures of MBE for AP (left), BP (middle), and GP (right) systems

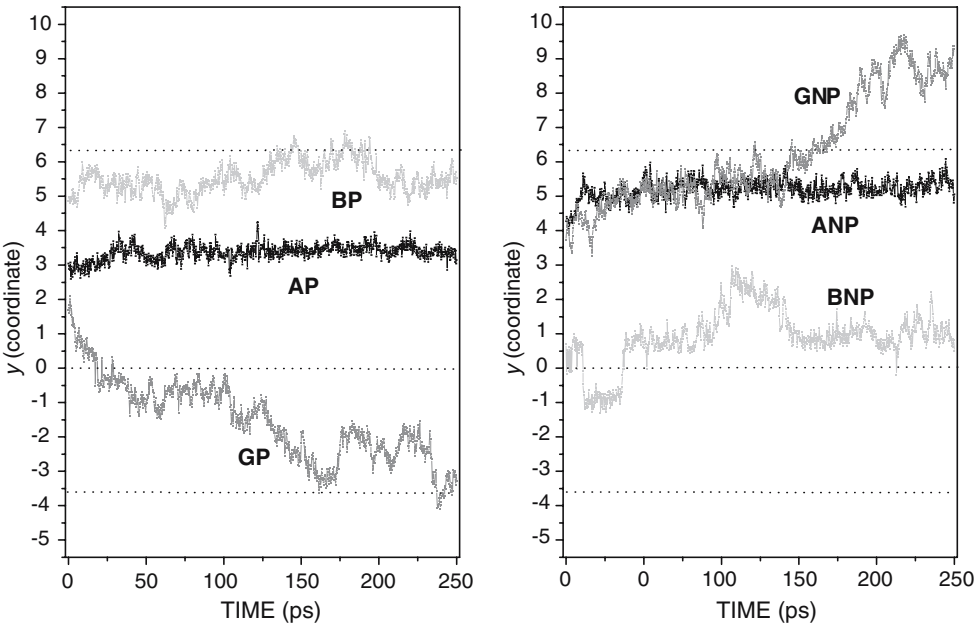

Fig. 6 History of the y coordinates of the center of mass of the naphthalene group of 2MN over a 250 ps MD trajectory at 300 K for six systems studied. Dashed lines are the y coordinate of the planes that contain the center of mass of: the C atoms of methyl end groups of hydroxypropyl chains (y = +6.3 Å); the bridging O atoms (y = 0); and the oxygens of primary OH at the opposite side (y = –3.6 Å) for the undistorted hosts

host and guest molecules. The average of both angles does not generally change much from the initial values (θ_{min} and ε_{min}). However, in some cases θ can fall into another local minimum during the MD trajectory, placed at $\theta_{min} \pm (360°/n)$, where n is the number of glucopyranose units.

Table 4 (rows 6 and 7) collects the average number of intramolecular hydrogen bonds for HPCD as well as the intermolecular ones between HPCD and the 2MN guest for the systems investigated. The number of intramolecular HBs of each HPCD obviously increases with the number of glucopiranose units in the HPCD. With regard to to the intermolecular HB (HPCD–2MN), two values stand out over the others, the ones for AP and BNP. These HB are due to interactions between the carboxylic oxygen from the 2MN guest and the primary OH(6) and OH at C2 of HP chain, respectively.

The negative average of binding energies for all systems indicates that the structures of 1:1 complexes are stable. Nevertheless, as with MM, the average of binding energies is again more favorable, with the exception of the BNP system, for P complexation. As previously with MM, binding energies become more negative as the HPCD macroring size decreases, the exception again being BNP systems. As previously,

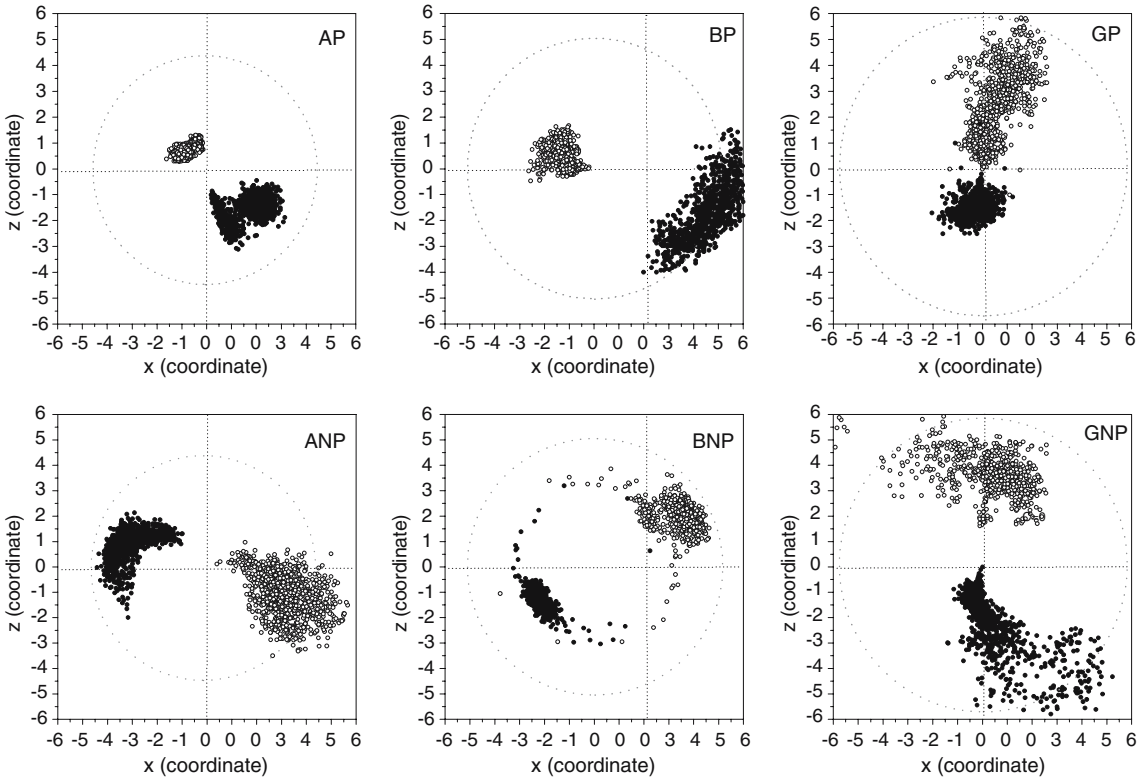

Fig. 7 Instantaneous *xz* projection, looking from the positive y coordinate side, of the placement of carboxylic oxygen (open circles) and H(5) (filled circles) atoms of the 2MN guest for all the systems studied. Dotted lines show the location of the bridging oxygen atoms rim for the non-distorted α-, *β*-, and *γ*-HPCDs with radii of ~4.4, 5.2, and 5.9 Å, respectively

most of the stabilization inside the HPCD cavity is due to van der Waals interactions. Electrostatics interactions always represent less than 20% of average binding energies. Table 4 also collects average non-bonded interaction energies between relevant groups of 2MN and modified HPCDs. Most of these results could be predicted, at least for the P approaching, by looking at the change upon complexation of the interaction energy contributions from Fig. 4 and the guest placements listed in row 2 of Table 4. The location of the guests is obviously a result of the balance between the different interaction energies. As with MM, the average of both naphthalene and ester/HPCD interactions always seems to be favorable to complexation. However, the amount of these contributions to the total average binding energy due to the ester group reaches the maximum values for AP and BP (34 and 39%, respectively) followed by BNP (24%). The total potential energy of the systems and all its contributions follow the predicted behavior, generally showing a parallel increase with system size. As with MM, strain is the most important contribution to the total potential energy, most of it due to the HPCD host.

Table 3 Average of the instantaneous rate (in Å/ps) of variation of *x, y*, and *z* coordinates for the heavy atoms (excluding H atoms) of the 2MN guest over the 0.25 ns MD trajectory for all studied systems

System	$\frac{\langle \Delta x_i \rangle}{\Delta t}$	$\frac{\langle \Delta y_i \rangle}{\Delta t}$	$\frac{\langle \Delta z_i \rangle}{\Delta t}$
AP	0.68	0.69	0.67
BP	0.75	0.75	0.78
GP	0.76	0.75	0.79
ANP	0.75	0.82	0.76
BNP	0.71	0.73	0.74
GNP	0.78	0.81	0.86

Concluding remarks

The MM and MD calculations reveal that the 1:1 inclusion complexes of the 2MN guest with HPCDs can feasibly form.

Although both P and NP approaches are energetically possible, several reasons that are in agreement with experiments lean toward a 2MN guest polar approach: (a) $E_{binding}$ obtained by MM and MD are generally more favorable for the P approach; (b) For the structures of MBE for AP, BP, and GP systems, the 2MN is placed in a very similar microenvironment,

Table 4 Average of some geometrical parameters, number of hydrogen bonds, binding energies (the electrostatics and van der Waals contributions), total energies, and contributions obtained from the analysis of 250 ps MD trajectories of different systems

Parameters	AP	BP	GP	ANP	BNP	GNP
y (coordinate) (Å)	3.4	5.5	–1.5	5.2	0.9	5.2
θ (°)	–46.5	–67.5	10.6	108.0	58.2	10.8
ε (°)	69.3	76.9	62.1	90.2	78.6	105.1
Number of HB						
Intra–HB_{HPCD}	4.86	7.00	7.05	5.61	6.43	8.20
Inter–$HB_{HPCD–2MN}$	0.37	0.03	0.19	0.00	0.70	0.11
Energy (kJ/mol)						
$E_{binding}$	–96.9	–60.1	–52.0	–51.0	–84.1	–37.3
Electrostatic part	–9.0	–4.3	–6.1	–9.7	–9.8	–5.5
van der Waals part	–87.9	–55.7	–45.9	–41.3	–74.3	–31.7
$E_{int\ HPCD–2MN\ naphthalene}$	–64.0	–36.7	–045.9	–47.5	–63.7	–34.2
Electrostatic part	–2.6	–4.0	–4.6	–8.3	–4.9	–5.3
van der Waals part	–61.4	–32.5	–41.3	–39.2	–58.8	–26.4
$E_{int\ HPCD–2MN\ ester}$	–32.9	–23.7	–6.1	–3.5	–20.4	–3.1
Electrostatic part	–6.5	–0.3	–1.5	–1.5	–4.8	–1.1
van der Waals part	–26.4	–23.2	–4.6	–2.1	–15.6	–2.9
E_{tot} guest : host	901.7	1081.9	1225.9	923.7	1070.3	1261.3
Electrostatic part	127.8	151.2	165.6	122.0	149.9	163.6
van der Waals part	–35.1	7.3	18.0	7.6	–8.10	46.4
Strain energy	796.6	911.3	1029.8	781.7	916.5	1032.4
E_{tot} host	872.8	1015.3	1152.6	848.5	1027.7	1176.3
Electrostatic part	98.8	117.7	134.0	93.9	122.1	143.6
van der Waals part	37.7	47.7	48.8	33.5	50.6	59.5
Strain energy	736.3	850.0	969.7	721.1	855.0	973.1
E_{tot} guest	125.8	126.6	125.3	126.1	126.8	124.3
Electrostatic part	38.0	37.8	37.7	37.9	37.6	37.7
van der Waals part	15.1	15.4	15.1	15.3	15.7	15.2
Strain energy	60.3	61.3	60.1	60.5	61.5	59.4

which is in agreement with the quencher measurements and the estimation of the polarity of medium surrounding the guest when complexed with any of HPCDs, which is very similar ($\varepsilon \approx 50$) [49]. This does not occur when 2MN approaches on the NP side. (c) The interaction of the 2MN ester group with the primary hydroxyl groups rim, which is an important contribution to $E_{binding}$, is larger for P systems. This is especially true for the 2MN : α-HPCD complex. This interaction, most of it probably due to hydrogen bonding, could explain a special behavior of fluorescence lifetime measurements when 2MN complexes with α-HPCD. This interaction should also contribute to significantly moderate the 2MN movement inside the cavity in agreement with the experimental entropy changes. According to MD results, this moderation does not occur when part of the 2MN is outside the cavity with the ANP system. (d) Experimental results of the complexation of 2,6-dimethyl naphthalene dicarboxylate, DMN (two ester groups instead of one) with α-CD, studied by us [47], proves the formation of very stable DMN : CD_2 complexes by complete penetration of both ester groups into both α-CDs. This fact corroborates that a polar side penetration is perfectly feasible for 2MN [47].

Complexation of HPCDs causes a decrease in the total potential energy of the system, where non-bonded van der Waals interactions are mainly responsible for such a decrease. These results contrast with the ones previously obtained for complexation of 2MN with the natural occurring α- and β-CDs that make E_{tot} increase, the strain term being responsible for this increment. These results are derived from the apparently wider entrance of the HPCD cavity when compared to their unsubstituted counterparts (F. Mendicuti, unpublished data).

$E_{binding}$ at the MBE or averaged values obtained by MD, when 2MN approaches by P side, follows the same trend as experimental enthalpy changes, becoming more negative as the HPCD size decreases.

Molecular dynamics results indicate that the mobility, translation or rotation inside the cavity, of the guest is smaller when 2MN is confined tothe narrow α-HPCD cavity than when it is in the β- or γ-HPCDs. The possibility of attractive 2MN-α-HPCD interactions (HB interaction) contributes in the same way. This fact

allows for the explanation of the signs of entropy changes upon binding.

Acknowledgments This research was supported by Comunidad de Madrid (CAM projects: GR/MAT/0810/2004; S–055/MAT/0227), CICYT (project CTQ2005-04710/BQU), and Universidad de Alcalá (grant to A.D.M.). We also express our thanks to M. L. Heijnen for assistance with the preparation of the manuscript.

References

1. Bender, M.L., Komiyama, M.: Cyclodextrins Chemistry, p. 34. Springer Verlag, Berlin (1978).
2. Szejtli, J.: Cyclodextrins and their Inclusion Complexes, p. 296. Akadémiai Kiadó, Budapest (1982).
3. Szejtli, J.: Cyclodextrin Technology, p. 450. Kluwer Academic Publisher, Dordrecht (1988).
4. Szejtli, J., Osa, T. (eds.): Comprehensive Supramolecular Chemistry: Cyclodextrins, vol. 3. Elsevier, Oxford (1996).
5. D'Souza, V.T., Lipkowitz, K.B.: Chem. Rev. **98**(5), 1741 (1998).
6. Harata, K.: Bull. Chem. Soc. Jpn. **49**, 197 (1976).
7. Tabushi, I., Kiyosuke, Y., Sugimoto, T., Yamamura., K.: J. Am. Chem. Soc. **100**(3), 916 (1978).
8. Ohashi, M., Kasatani, K., Shinohara, H., Sato, H.: J. Am. Chem. Soc. **112**, 5824 (1990).
9. Menger, F.M., Sherrod, J.: J. Am. Chem. Soc. **110**, 8606 (1988).
10. Venanzi, C.A., Canzius, P.M., Zhang, Z., Brunce, J.D.: J. Comput. Chem. **10**, 1038 (1989).
11. Ohashi, M., Kasatani, K., Shinohara, H., Sato, H.: J. Am. Chem. Soc. **112**, 5824 (1990).
12. Jaime, C., Redondo, J., Sánchez, F., Sanchez-Ferrando, F., Virgili, A.: J. Org. Chem. **55**, 4772 (1990).
13. Jaime, C., Redondo, J., Sánchez, F., Sanchez-Ferrando, F., Virgili, A.: J. Mol. Struct. **248**, 317 (1991).
14. Sherrod, M.J.: In: Davies, J.E.D. (ed.) Spectroscopic and Computational Studies of Supramolecular Systems, p. 187. Kluwer Academic, Dordrecht (1992).
15. Lipkowitz, K.B., Roghothama, S., Yang, J.: J. Am. Chem. Soc. **114**, 1554 (1992).
16. Köhler, J.E.H., Hohla, M., Richters, M., König, W.A.: Angew. Chem. Int. Ed. Engl. **31**, 319 (1992).
17. Amato, M.E., Djedaïni-Pilard, F., Perly, B., Scarlata, G.: J. Chem. Soc. Perkin Trans. **2**, 2065 (1992).
18. Amato, M.E., Pappalardo, G.C., Perly, B.: Magn. Reson. Chem. **31**, 455 (1993).
19. Kobor, F., Angermind, K., Schomburg, G.: J. High Resol. Chrom. **16**, 299 (1993).
20. Fotiadu, F., Fathallah, M., Jaime, C.: J. Incl. Phenom. Mol. Rec. Chem. **16**, 55 (1993).
21. Fathallh, M., Fotiadu, F., Jaime, C.: J. Org. Chem. **59**, 1288 (1994).
22. Mark, E., van Helden, S.P., Smith, P.E., Janssen, L.H.M., van Gunsteren, W.F.: J. Am. Chem Soc. **116**, 6293 (1994).
23. Amato, M.E., Lombardo, G.M., Pappalardo, G.C., Scarlata, G.: J. Mol. Struct. **350**, 71 (1995).
24. Berg, U., Gustavsson, M., Aström, N.: J. Am. Chem. Soc. **117**, 2114 (1995).
25. Kano, K., Kato, Y., Kodera, M.: J.Chem. Soc. Perkin Trans. **2**, 1211 (1996).
26. Amato, M.E., Lipkowitz, K.B., Lombardo, G.M., Pappardo, G.C.: J.Chem. Soc. Perkin Trans. **2**, 321 (1996).
27. Black, D.R., Parker, C.G., Zimmerman, S.S., Lee, M.L.: J. Comp. Chem. **17**, 931 (1996).
28. Jursic, B.S., Zdravkovski, Z., French, A.D.: J. Mol. Struct. (Theochem) **366**, 113 (1996).
29. Salvatierra, D., Jaime, C., Virgili, A., Sanchez-Ferrando, F.: J. Org. Chem. **61**, 9578 (1996).
30. Cozzini, P., Domiao, P., Musini, P.C., Palla, G., Zanardi, E.: J. Incl. Phenom. Mol. Rec. Chem. **26**, 295 (1996).
31. Maletic, M., Wennemers, H., McDonald, D.Q., Breslov, R., Still, W.C.: Angew. Chem. Int. Ed. Engl. **35**, 1490 (1996).
32. Ivanov, P.M., Salvatierra, D., Jaime, C.: J. Org. Chem. **61**, 7012 (1996).
33. Salvatierra, D., Sánchez-Ruiz, X., Garduño, R., Cervelló, E., Jaime, C., Virgili, A., Sanchez-Ferrando, F.: Tetrahedron **56**, 3035 (1996).
34. Lipkowitz, K.B., Pearl, G., Coner, B., Peterson, M.A.: J. Am. Chem Soc. **119**, 600 (1997).
35. Lipkowitz, K.B.: Chem. Rev. **98**(5), 1829 (1998).
36. Dodziuk, H., Kozminski, W., Lukin, O., Sybilska, D.: J. Mol. Struct. (Theochem) **525**, 205 (2000).
37. Dodziuk, H., Lukin, O., Nowinski, K.S.: J. Mol. Struct. (Theochem) **503**, 221 (2000).
38. Lino, A.C.C., Takahata, Y., Jaime, C.: J. Mol. Struct. (Theochem) **594**, 207 (2002).
39. Grabuleda, X., Ivanov, P., Jaime, C.: J. Org. Chem. **68**, 1539 (2003).
40. Madrid, J.M., Pozuelo, J., Mendicuti, F., Mattice, W.L.: J. Colloid Interface Sci. **193**, 112 (1997).
41. Pozuelo, J., Mendicuti, F., Mattice, W.L.: Macromolecules **30**, 3685 (1997).
42. Madrid, J.M., Mendicuti, F., Mattice, W.L.: J. Phys. Chem. B **102**, 2037 (1998).
43. Pozuelo, J., Mendicuti, F., Mattice, W.L.: Polym. J. **30**, 479 (1998).
44. Madrid, J.M., Villafruela, M., Serrano, R., Mendicuti, F.: J. Phys. Chem. B **103**, 4847 (1999).
45. Pozuelo, J., Nakamura, A., Mendicuti, F.: J. Incl. Phenom. Macroc. Chem. **35**(3), 467 (1999).
46. Pozuelo, J., Mendicuti, F., Saiz, E.: In: Labandeira, J.J., Vila, J.J. (eds.) Proceedings of the 9th International Symposium on Cyclodextrins, p. 567. Kluwer Academic, The Netherlands (1999).
47. Cervero, M., Mendicuti, F.: J. Phys. Chem. B **104**, 1572 (2000).
48. Pastor, I., Di Marino, A., Mendicuti, F.: J. Phys. Chem. B **106**(8), 1995 (2002).
49. Di Marino, A., Mendicuti, F.: Appl. Spectrosc. **56**(12), 1579 (2002).
50. Madrid, J.M., Mendicuti, F.: Appl. Spectrosc. **51**, 1621 (1997).
51. Clark, M., Cramer, R.C. III, Van Opdenbosch, N.: J. Comp. Chem. **10**, 982 (1989).
52. Sybyl 6.9, Tripos Associates, St. Louis, Missouri, USA.
53. MOPAC (AM1) Included in the Sybyl 6.9 package.
54. Brunel, Y., Faucher, H., Gagnaire, D., Rasat, A.: Tetrahedron **31**, 1075 (1975).
55. Press, W.H., Flannery, B.P., Teukolski, S.A., Vetterling, W.T.: Numerical Recipes: The Art of Scientific Computing, p. 312. Cambridge University Press, Cambridge, MA (1988).
56. Blanco, M.: J. Comp. Chem. **12**(2), 237 (1991).